Anchor Damage to Offshore Cables

by Michael Hoffman (K)

Fourth-year undergraduate project
in Group D, 2013/2014

I hereby declare that, except where specifically indicated, the work submitted herein is my own original work.

Signed:

Michael Hoffman

Date: 25-05-2014

Technical abstract

Worldwide there are over a million kilometers of subsea cables which are used for telecommunications and increasingly as electrical connections both between countries and between offshore renewable energy sources and power grids. Subsea cables are therefore fundamental to modern society and breakage of cables can lead to large scale disruption and financial losses for both individuals and whole economies. One of the major causes of breakage is anchors being deployed on to or being dragged through a cable, to protect against this, cables are often buried in the seabed. However the existing guidelines are largely qualitative, don't quantify soil strength or allow a suitable burial depth to be chosen for a specific anchor size.

This report details the design and use of an experimental setup to collect quantitative data on the maximum penetration depth of anchors in soils of varying strengths. This data is then used to produce a design burial depth chart for subsea cables in soft clay soils.

Based on background reading a Danforth anchor was modelled being dragged through normally consolidated Kaolinite clay behind a vessel, as one of the largest anchors used on the continental shelf it gives an upper bound on expected penetration depths, leading to conservative burial depths. This was achieved using an actuator and guides to pull the model anchor around the circumference of a mini-drum centrifuge; by rotating the centrifuge at different speeds the necessary laboratory scaling and stress history could be achieved.

Nine experiments were carried out, the first four did not yield results but valuable lessons were learnt that enabled a reliable experimental procedure and setup to be developed. As a result of this development five successful experiments were carried out and results obtained. These experiment consolidated the Kaolinite at an centrifugal acceleration of 40g and 80g and tested at an acceleration of 10g, 20g and 40g; producing two different undrained soil strength profiles and testing anchors with prototype weights of 35kg, 280kg and 2240kg respectively.

Analysis of the soil strength profiles of consolidated samples shows linearly increasing undrained shear strength with depth as expected for normally consolidated soils. The prototype undrained shear strength gradients obtained at 80g and 40g were $\frac{100}{N}$kPa/m and $\frac{33.4}{N}$ kPa/m respectively, where N is the test speed (N g). A comparison of these gradients at 10g, 20g and 40g is made with measurements in the Nile delta and North Sea and it is concluded that the centrifuge modelling accurately represents soft clay seabeds.

Dimensional analysis of the problem yielded three dimensionless groups: $\frac{d}{L}$; $\frac{K_{S_U} L^3}{mg}$ and $\frac{\rho_s L^3}{m}$. Where m is the anchor mass, d the maximum penetration depth, L the anchor shaft length and K_{S_U} the undrained shear strength gradient. The experimental results are plotted on a graph of $\frac{d}{L}$ against $\frac{K_{S_U} L^3}{mg}$ where $\frac{\rho_s L^3}{m}$ is a constant. All points are found to lie along the line:

$$\frac{d}{L} = -0.0545 \times \frac{K_{S_U} L^3}{mg} + 0.8422$$

As can be seen, this equation correctly models anchor behaviour; heavier anchors penetrate deeper than lighter anchors and the penetration depth in a weaker soil is greater than that in a stiffer soil.

Analysis of both penetration depth readings and observations leads to the conclusion that the anchor penetrates to an equilibrium depth where it moves with the anchor flukes parallel to the soil surface. This is in agreement with numerical models for drag anchors used for offshore mooring. Using this finding, a mathematical model of the anchor is produced and the resultant penetration depths compared to the experimental results and an empirical model used for drag anchors. It is found that the empirical model gives misleading results and a comparison between Danforth and drag anchors cannot be made. The mathematical model more accurately represents the experimental findings but tends to overestimate penetration depths in softer soils and underestimate penetration depths in stiffer soils.

Following this modelling, a comparison is made between the experimental penetration depths and static penetration depths as predicted by shallow foundation bearing theory. It is found that anchors penetrate at least twice as deep when experiencing a horizontal force, corroborating the model established earlier. In addition, tensile tests of the anchor cable and investigations into the tendency of the model to rotate are detailed. It is found that both the anchor rode breaking and the anchor rotating are due to small inaccuracies in the experimental model and adjustments are suggested.

Further improvements to the apparatus are then discussed, primarily the need for a more accurate measurement of the undrained shear strength. The need for more experimental results, over a larger range of soil strength profiles, anchor weights and anchor types is then highlighted.

In conclusion, the design line established in this project allows the required burial depth for subsea cables to be calculated in order to protect them from damage by anchors being dragged behind ships. This is a conservative design line however it enables more effective burial than using net burial depths. This can lead to cost and emissions savings over the whole life of the project making cable burial more sustainable. Based on this line, the existing guideline for burial in soft clays is found to be overly conservative by a factor of two. This finding is in agreement with actual trials carried out in German Bight which suggest the existing guidelines for fine sand are also overly conservative by a factor of two. As a result a new design chart for cable burial in soft clay is suggested as shown in figure 1.

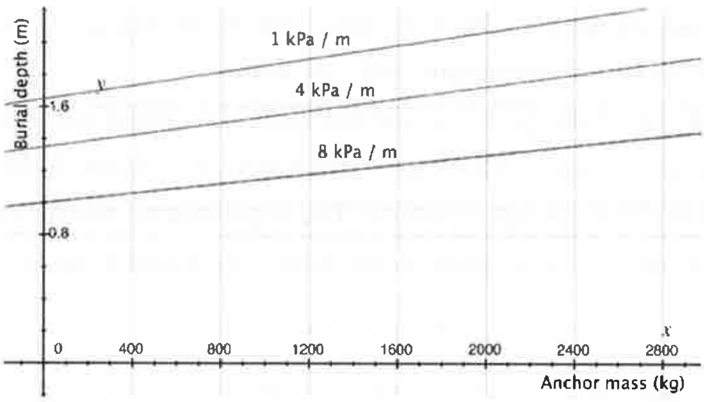

Figure 1: Proposed design chart for determining safe cable burial depth in soft clays

Contents

1 Introduction 3

2 Theory and design of experiment 6

2.1 Deployment of anchors 6

2.2 Cable burial 7

2.3 Centrifuge modelling 8

2.3.1 Scaling laws 8

2.3.2 Limitations of centrifuge modelling 9

3 Apparatus 11

4 Experimental technique 14

4.1 Experimental method 14

4.2 Experimental accuracy 16

5 Results and discussion 16

5.1 Experiment reports 16

5.2 Soil profiles 19

5.2.1 Experimental soil profiles 19

5.2.2 Shear strength profiles of real seabeds 21

5.3 Penetration readings 21

5.3.1 Anchor behaviour 22

5.3.2 Dimensional analysis 23

5.3.3 Mathematical modelling of anchor penetration 27

5.3.4 Anchor twisting 32

5.3.5 Anchor rode tensile strength 32

5.3.6 Static and dynamic penetration depth comparison 33

5.4 Future experimentation 35

6 Conclusions 35

7 Bibliography 38

8 Appendix I 40

8.1 Calculation of error 40

9 Appendix II 41

9.1 Experiment 5 observations and readings 41

9.2 Experiment 6 observations and readings 42

9.3 Experiment 7 observations and readings 43

9.4 Experiment 8 observations and readings 44
9.5 Experiment 9 observations and readings 45

10 Appendix III **46**
10.1 Comments on initial risk assesment 46

1 Introduction

Worldwide there are over 1 million km of subsea cables [1]; most subsea cables are fibre-optic and carry 95% of worldwide telecommunications [2]. With the growth of off-shore renewable energy systems such as the planned 339 turbine Moray Firth wind farm, the largest to date which is scheduled to start construction in 2015 [3], the number of subsea telecommunications and power cables is set to increase greatly.

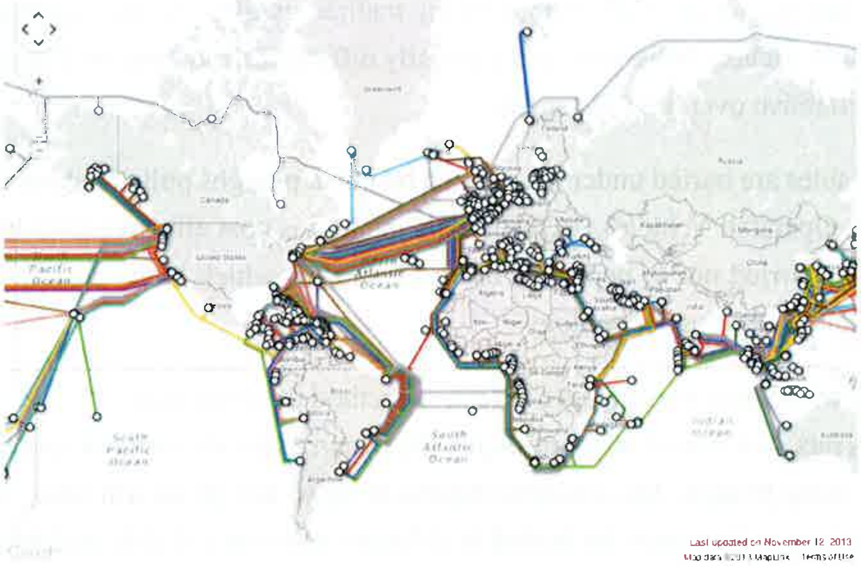

Figure 1: Map of major submarine cables [4]

Current records show an average of 0.1 faults per 1000km of subsea cable every year due to external aggression [5]. Of these faults 17-19% [5] are caused by anchors catching onto or cutting through cables. Anchors therefore cause an average of 18 faults per year worldwide. Although this is a relatively small number they are expensive and time consuming to repair.

Repair of a cable fault begins with its detection by the service provider who then identifies the exact location electronically and mobilises the nearest available cableship. The mobilised cableship then cuts and lifts the cable ends before replacing the damaged length and splicing the resultant ends back together. This process can take several weeks due to the large distances that need to be travelled and is an expensive operation; the 2001 Atlantic Cable Maintenance Agreement service contracts cost in excess of $60M per annum [6].

However the most damaging impact of a cable fault is the loss of telecommunications to local economies, on 30th January 2008, damage to the SeaMeWe 4 Cable outside of Alexandria Port affected an estimated 60M users in India, 12M in Pakistan, 6M in Egypt and 4.7M in Saudi Arabia [7]. The true cost of this break to the individuals and economies concerned is significant but unquantifiable, it is therefore vitally important to protect subsea cables from damage caused by anchors.

Anchors cause damage by being deployed onto or near a subsea cable, the forces of the wind and waves can then move the vessel, which drags the anchor along through the seabed. If the anchor is dragged across a cable it either shears or bends the cable; due to the brittleness of glass fibres, even a gentle bend is sufficient to snap the fibres. There are currently three methods used to protect cables from damage:

1. Armouring the cable - cables are wrapped in additional layers of steel reinforcement, this is costly and provides minimal protection against most large anchors.

2. Rock mattresses - cables are buried under mattresses of rock, this provides protection against most anchors however it is logistically difficult to carry out in deeper water and is not cost effective over long distances.

3. Burial - cables are buried under the sea bed by cable ploughs pulled behind a cableship or Remotely Operated Vehicles (ROVs). This method is cost effective over large distances and can be carried out to depths of up to 1500m [8] which is the current limit of most trawling and anchoring technology.

Burial is therefore the only existing cost-effective method of protection.

For many years, net burial at 0.6m depth [9] occurred in all areas of concern but more recently burial using ploughs has achieved depths of up to 4m [8] in soft soils. In an attempt to specify how deep cables must be buried in different soil types, Cable and Wireless Marine created the Burial Protection Index (BPI) [10], as shown in figure 2. This index is largely qualitative; soils are classified by type as opposed to strength, there is no allowance for the type of anchor and the burial depths are based upon cable plough penetration data as opposed to anchor penetration data. Therefore this index is not sufficient to identify the depth at which a subsea cable must be buried to provide protection from a specific anchor in a specified soil and thus effectively plan a cable route.

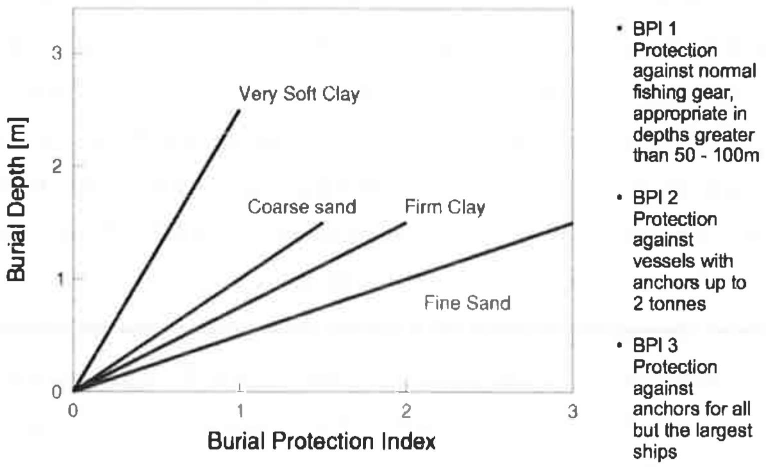

Figure 2: Graph of Burial Depth against Burial Protection Index

Development of new wind farms in German Bight initially required cable burial depths of 3m in shipping channels and 1.5m outside of these channels. Due to excessive costs and the technological challenges a trial was set up by the German Coastal Department to establish whether these depths were suitable. The trial involved deploying and dragging anchors in three different sites and using sonar, sediment echosounder surveying (SES) and visual inspection using ROVs to determine their embedment depth as shown in figure 3. Two types of anchor were used, an 11.7 tonne Hall anchor and a high holding power (HHP) APC 14 weighing approximately 8.3 tonnes, both of which are comparable to a Danforth anchor. The series of 18 pulls yielded maximum recorded penetration depths of 0.67m for the HHP anchor and 0.88m for the Hall anchor, as shown in figure 4[11]. However these tests were only carried out on very specific sandy seabeds, the results do not attempt to quantify penetration in terms of soil density or anchor weight and are only applicable for the sampled areas as shown in figure 4.

The three areas investigate consisted of loose fine sand (Nord, yellow in figure 4), medium dense sand with some silt (Sud, green) and densely packed sand (VTG, blue). As can be seen in figure 4, the greatest penetration depth occurs in the loosest sand, with the APC 14 anchor achieving 0.69m penetration and the Hall anchor achieving 0.88m. Conversely, the densest sand gave smaller penetration depths of 0.34m and 0.28m for the APC 14 and Hall anchors respectively. Using the BPI design chart, to protect from anchors of this size (BPI 3), burial at a depth of 1.5m is suggested in fine sands. This suggests that BPI is conservative by a factor of at least 2 for fine sand.

Figure 3: Picture of Sonar and SES ships from offshore tug dragging an anchor behind it [11]

Position	Ankertyp	tracklength	Max. pull	Max. Δ z
		[m]	[t]	[m]
N1	AC14	67	62	0.65
N2	Hall	92	64	0.70
N3	AC14	57	82	0.69
N5	Hall	87	58	0.88
N6	Hall	92	65	0.78
S1	AC14	63	86	0.33
S2	AC14	20	95	0.28
S3	AC14	102	64	0.34
S4	Hall	23	76	0.28
S5	Hall	27	72	0.28
S6	Hall	22	80	0.26
V1	AC14	107	73	0.33
V2	Hall	27	75	0.34
V3	AC14	20	78	0.19
V4	Hall	24	79	0.26
V5	AC14	31	80	0.67
V6	Hall	26	80	0.67

Figure 4: Measured anchor penetration depths [11]

Extensive physical, numerical and analytical modelling as well as in-situ testing has been undertaken to quantify the behaviour of drag anchors. These large anchors are designed to embed into the soil and act as mooring points for large offshore structures [12]. As discussed in section 5.2.2, there are some limited similarities between drag anchor and ship anchors, however the extreme difference in size means accurate extrapolation of these results for ship anchors is not possible.

The aim of the project is therefore to design and build an experimental rig and use it to collect quantitative experimental data to describe the maximum embedment depth of ship anchors in soils of varying strengths. This data can aid in the selection of burial depths for cables to suit their planned route, maximising the protection provided from burial whilst minimising the cost of installation and maintenance.

2 Theory and design of experiment

2.1 Deployment of anchors

Anchors come in varying forms with a large variety of fluke designs and a range of sizes to facilitate anchoring in different soil conditions for various sizes of ship, as shown in figure 5.

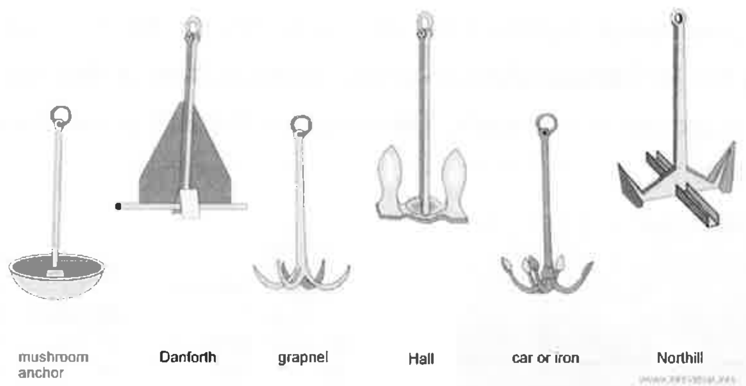

Figure 5: Common anchor types [14]

Anchors are attached to the vessel by a rode of length 7-10 times the expected anchoring water depth. The initial 2-12.5m of rode nearest the anchor is chain link with the remaining length being composed of rope [13].

Deploying an anchor involves lowering the anchor to the seabed and releasing an additional length of rode equal to 5-10 times the water depth. This additional length of rode allows the vessel to move downwind of the anchor, the combination of long rode and heavy chain near the anchor produces a catenary shape as shown in figure 6. As a result, any load applied by the wind or tides to the vessel is transferred along the anchor rode and exerts an approximately horizontal force on the anchor. This is beneficial as the horizontal resistance provided by a soil is much greater than that offered to a vertical force, therefore the anchor can withstand much greater forces. Conversely, to raise the anchor, the vessel moves into location above the anchor, and draws it up vertically, taking advantage of the smaller vertical resistance.

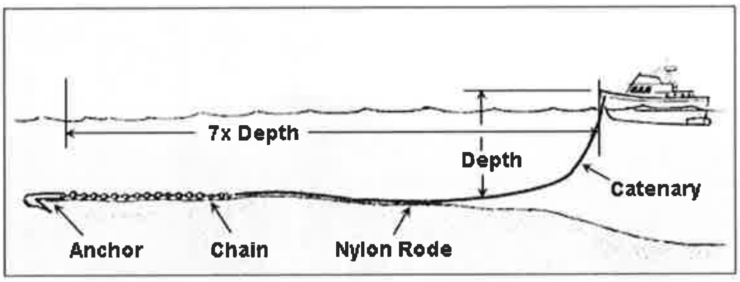

Figure 6: Diagram of a deployed anchor [15]

As most anchor damage is caused by anchors being dragged along the sea bed when fully deployed, ie. when the horizontal forces acting on an anchor are greater than the resistance offered by the soil, this experiment aims to replicate the behaviour of an anchor being dragged when fully deployed.

To make the results as useful as possible the experiment aims to model the anchors that most commonly cause faults. Over 70% of anchor related faults occur in water less than 50m deep [9] which is most commonly used by fishing vessels. To find an upper bound on the penetration depth of anchors the Lloyd's Register Rules and Regulations for the Classification of Ships [13] was used to identify a 225kg anchor as the largest, most commonly used anchor size in this area. In addition a Danforth type anchor was identified as resulting in the deepest penetration of all common anchor types. The dimensions of this anchor can be obtained from any shipping supplies retailer [16]. The Lloyd's register then identifies a suitable rode to be composed of 3m of studless chain with a total length in excess of 7 times the water depth [13]. A scale model of this anchor and rode are therefore to be used in all experimentation.

2.2 Cable burial

As identified in section 1, cable burial is the only cost effective method of protecting subsea cables. The three main methods of installation are: using ROV's fitted with jetting tools that cut away clay and fluidise sand to produce a trench 20-40cm wide; displacement cable ploughs which cut open a V-shaped trench up to 5m wide and non-displacement ploughs which use a thin blade to produce a thin slit between 30cm and 1m wide into which a cable can be inserted [17].

As shown in figure 7, the soil removed is often not replaced above the cable by the plough or ROV, however trench collapse and sedimentation will fill it in with loose material over time. Additionally, as anchors will most likely approach from the side of a cable the soil directly above has little affect on the resultant behaviour.

The excavation method used by displacement ploughs doesn't replace soil and is therefore likely to reduce the horizontal total stress around the cut, in saturated sand this will lead to a decreased effective stress and strength almost immediately whereas in clay the decrease in strength

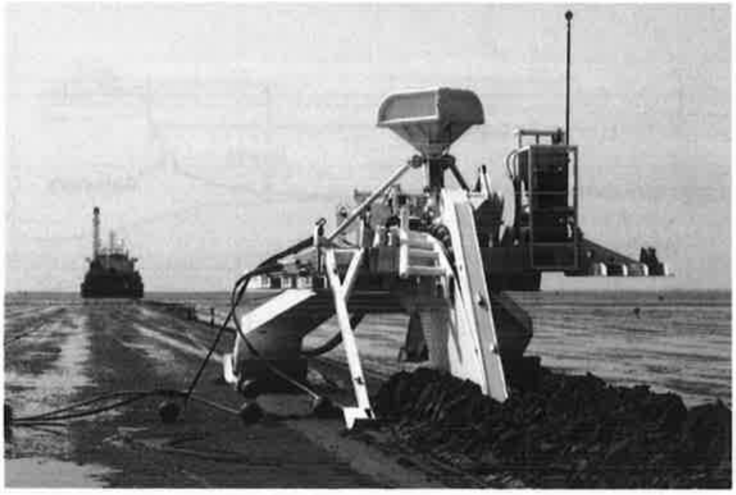

Figure 7: Picture of a cable plough operating on a beach [17]

and effective stress will occur over a period of hours to weeks depending on the permeability of the clay and depth of cut. Conversely non-displacement ploughs shear the soil. In stiff clay shearing can lead to a slight negative excess pore pressure near the cut due to dilation of the clay and a positive excess pore pressure further away from the cut. Over time equalisation will occur and the effective stress and strength of the soil surrounding the cable will increase slightly. In softer clay, contraction when shearing will result in a much larger increase in strength as equalisation occurs. However the cut is both shallow, in soft surface soils and only affects soil in the vicinity of the cable, it will therefore not offer the cable much extra protection against anchors. Similarly, jetting methods cause local, temporary increases in effective stress that will not lead to increased protection of the anchor.

If the clay is replace above a cable there is also no significant increase in strength. This is corroborated by in-situ testing using cone penetrometers in the Nile delta both before and after trenching. It was found that there was a 'similar range' of shear strengths measured both before and after trenching and backfilling [18].

To establish an upper bound on the penetration depth of anchors it is therefore conservative to assume that the soil around and above a cable has the same properties as the surrounding in-situ soil. By neglecting any potential increases in strength due to the installation process an upper bound on the penetration depth of anchors can be found.

2.3 Centrifuge modelling

2.3.1 Scaling laws

Centrifuge models are rotated at high speed so as to impose increased 'gravitational' acceleration upon physical models, allowing the model (m) to experience the same stresses as a full scale prototype (p). As a result, all lengths, mass and gravity scale as:

$$L_m = \frac{L_p}{N} \; ; M_m = \frac{M_p}{N^3} \; ; a_m = Na_p$$

Where N is the number of times greater the imposed acceleration is than normal gravitation acceleration, g. Therefore the effective stress experienced at 0.1m depth in a 50g centrifuge model equals the effective stress in a similar subsea location at 5m depth. Similarly a prototype anchor weighing 2 tonnes can be modelled by a 1:50 scale replica weighing 16 grams.

As anchor damage to offshore cables occurs in shallow and intermediate water depths, with anchor penetration depths in excess of 2m and drag distances in excess of 100m, scale modelling is required. A suitable method uses a 1m diameter drum centrifuge; allowing soil depths of up to 12m and drag distances of up to 240m to be modelled under a layer of water using anchors weighing in the order of 10 grams [19].

2.3.2 Limitations of centrifuge modelling

The aim of centrifuge modelling is for the dominant affect on the model to be the centrifugal acceleration, however several other forces act on the model.

Affect of variation in acceleration through the model

The gravity field in a centrifuge varies with the radius as $Ng = \omega^2 r$, where r is the radial distance and ω is the rotational speed. The result is that the surface of the model, closer to the centre, experiences slightly less acceleration than the nominal and the bottom slightly more. Based on findings by Taylor [19], the experienced gravitational field in a model of height h corresponds exactly to that of the prototype at two-thirds depth, he then derives that the effective centrifuge radius should be measured from the central axis to one third of the depth of the model as shown in figure 8. This corresponds to an effective radius of 0.4m in this experimentation. Based on a total model height of 0.15m, the ratio of maximum under/over - stress to the prototype stress is (r_u, r_o respectively):

$$r_u = r_o = \frac{h_m}{6R_e} = 0.0625$$

This variation is notable, however the experiment is designed for the anchor to penetrate the soil and find an equilibrium depth at approximately R_e. In addition to this, the magnitude of the maximum experimental error in the shear strength readings is also of this magnitude, it is therefore considered acceptable at this stage in the investigation.

Affect of the earths gravitational field

The acceleration experienced by the model is also affected by the earth's gravitational field. This field acts vertically downwards on all the material in the drum centrifuge whereas the major imposed acceleration is in the horizontal direction and is at least a factor of 10 greater that the earth's gravitational field. It is impossible to eliminate the affect of the earth's gravitational field however it is generally accepted that it is so small in comparison to the test speed that it can be

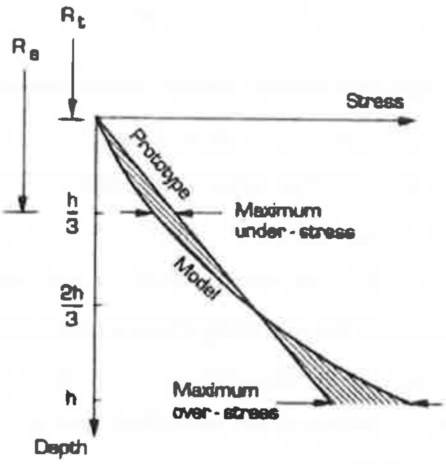

Figure 8: Comparison of stress variation with depth in a centrifuge model and its corresponding prototype [19]

neglected as is applied here. One possible result is that the anchor may tend to follow a slight downwards path but this will not affect the experimental results.

Affect of radial acceleration

In polar coordinates the radial acceleration for circular motion has the following form:

$$a_r = r\ddot{\theta} + 2\dot{r}\dot{\theta}$$

The experiment is carried out when the centrifuge's rotational speed has stabilised and the anchor is dragged at a relatively slow constant speed completing one rotation for every 300 of the centrifuge at 40g, therefore $\ddot{\theta}$ is negligible and the first term has no affect.

The second term is the coriolis term. The anchor penetrates the soil at a slow rate; from observations the penetration occurs in the first 10cm of the 1m drag distance so takes approximately 3s to occur and is to a maximum depth of 0.057m. As a result $\dot{r} = 0.019ms^-1$. Based on the above, the rotational velocity of the anchor itself is the rotational velocity of the experimental rig plus it movement relative to the rig. Based upon the above the anchors movement relative to the rig is 0.83 radians / s. The resultant radial acceleration is $a_r = 0.03154ms^-2$. This is less than 0.03 % of the smallest constant centrifugal acceleration used and is therefore negligibile.

Affect of soil particle size

Based on the scaling laws in section 2.3 it is logical to assume that the clay particles must be scaled in size by N. However there are no minerals with the same stress strain characteristics as clay with particles sufficiently small to allow testing at 40g. As a result the clay particle size isn't scaled, however Kaolinite has a particle size in the order of a few micrometers whereas the anchor size is of tens of millimeters. The factor 10,000 difference is considered sufficient to assume that the soil behaves like a continuum as it would in the prototype.

3 Apparatus

Based upon the above theory, experimental apparatus has been designed to model a 225kg Danforth anchor being dragged behind a vessel by producing a scale model, located inside the Schofield centre's 1m diameter mini-drum centrifuge (figure 9).

The experiment will measure the maximum penetration depth of the anchor in clay soils with differing strength profiles. Based on the assumption that burial of cables offers protection by isolating cables away from anchors as opposed to acting as a physical barrier, these upper bound penetration depths represent the minimum depth a cable must be buried to ensure its safety. The apparatus is to be arranged as shown in figure 10, a brief description of each piece of apparatus and its function is then given.

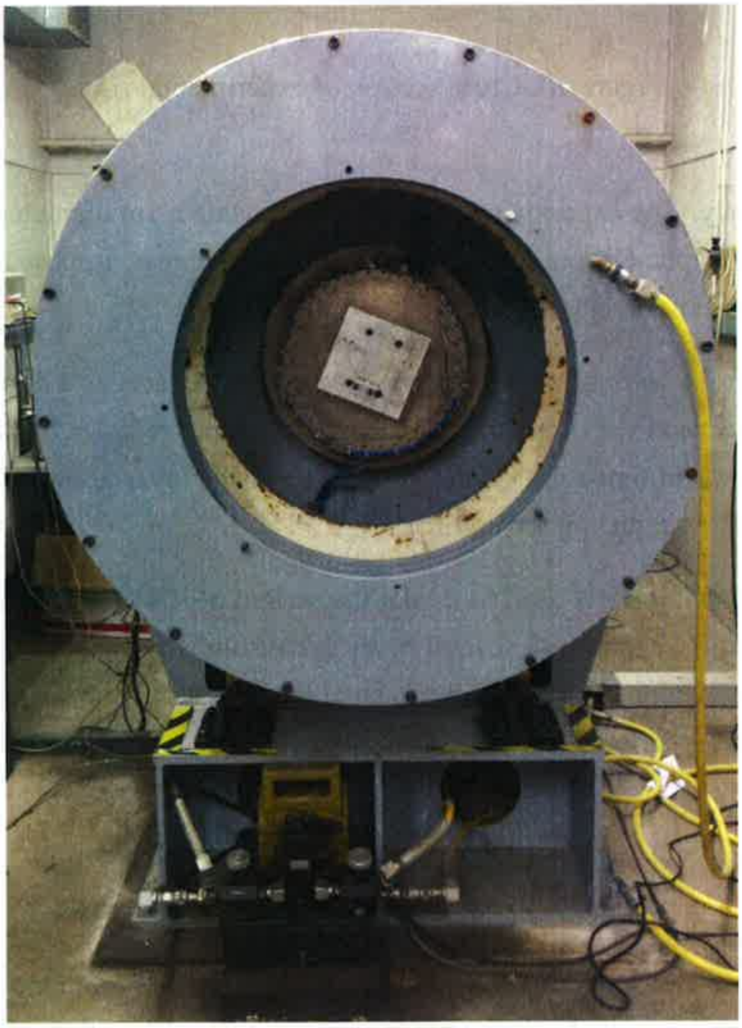

Figure 9: Mini-drum centrifuge based in the Schofield centre

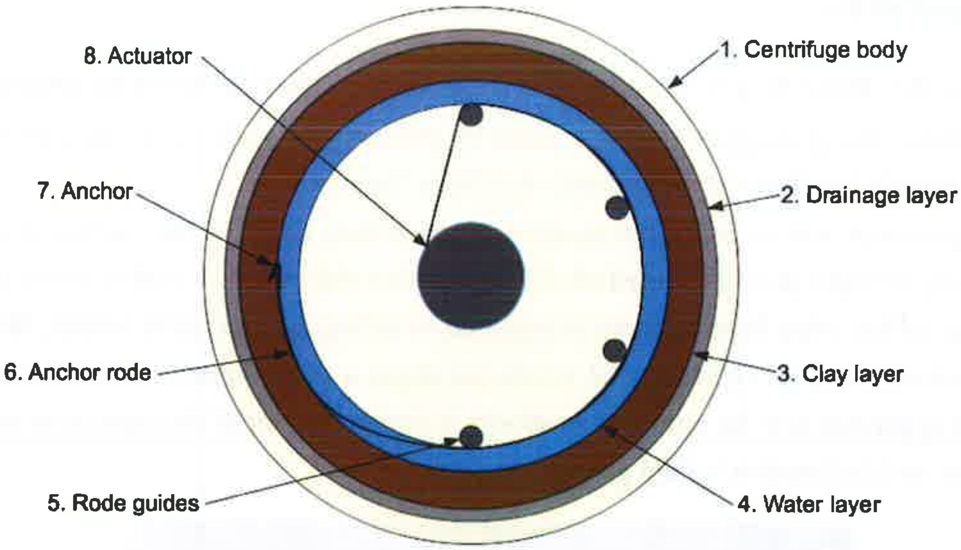

Figure 10: Cross section of experimental rig

1. Centrifuge body. The experimental rig is located inside a 1m diameter drum that rotates in the horizontal plane about its central axis and can therefore impose accelerations of up to 100g on the experimental model.

2. Drainage layer. A layer of geomembrane covered geonet acts as a drainage layer around the circumference of the drum and is connected to drainage holes leading out of the centrifuge as shown in figure 11. The additional drainage layer allows the clay samples to consolidate faster, reducing set-up time.

3. Clay layer. Kaolin clay is used to model the seabed, it is introduced as a slurry into the rotating centrifuge and left for several hours to consolidate. Once the clay is consolidated the centrifuge is stopped and the experimental rig is installed, the centrifuge is once again rotated and the experiment carried out.

4. Water layer. A thin layer of water is required on the surface of the clay to ensure the clay is saturated, this layer is controlled by water taps and standpipes attached to the centrifuge drum.

5. Rode guides. Steel rods bolted onto the drum around the circumference of the water layer ensure the anchor is pulled in a direction tangential to the drum, thus accurately modelling a vessel on the water surface dragging its anchor as shown in figure 12.

6. Anchor rode. A scale model of an anchor cable composed of 3m of studless chain between the anchor and main cable with a total length in excess of 7 times the water depth.

7. Anchor. A 1:25 scale model of a 225kg Danforth anchor is used for all testing (based on a model acceleration of 25g) as shown in figure 13.

8. Actuator. A large servo motor is attached to the centre of the rotating drum, this actuator rotates a pulley which winds up the anchor rode, dragging the anchor through the sea bed as shown in figure 14.

Figure 11: Drainage layer

Figure 12: Rode guides

Figure 13: Anchor

Figure 14: Actuator

Figure 15: Picture of experimental apparatus during an experiment

4 Experimental technique

4.1 Experimental method

The following experimental method was carried out:

1. Drainage layer placed into base of centrifuge channel and taped into place.
2. Safety screen bolted into place.
3. Centrifuge run at consolidation speed and clay slurry poured in through funnel and spreader as shown in figures 16 and 17.
4. Surface of clay measured using strobe light and scale draw onto the drum.
5. Clay allowed to consolidate until all visible primary consolidation had ceased.
6. Centrifuge stopped and spreading device removed.
7. Actuator, rode guides and anchor located in the drum as sown in figure 10.
8. Pasta inserted radially into clay as shown in figure 18.
9. Centrifuge spun at test velocity.

10. Actuator run for approximately 30s to drag anchor around half the circumference of the centrifuge, monitored visually using a strobe light.
11. Actuator and centrifuge stopped, safety screen removed.
12. Soil shear strength tests taken at increasing depths using a shear vane.
13. Depth of fluke tips below surface of clay measured using a ruler, extra shear strength measurements taken at this depth.
14. Clay excavated around broken pasta and penetration dpeth measurements from the clay surface taken using a ruler.
15. Apparatus rearranged to carry out an experiment over the other half of the circumference.
16. See 8.

Figure 16: Clay spreader funnel

Figure 17: Spreader device mounted in centrifuge

Figure 18: Spatial location of pasta and penetration depth measurement

4.2 Experimental accuracy

All penetration depth measurements were made with a ruler and are accurate to $+/-$ 0.5mm. However measurements made in the clay were subject to some human error as it was difficult to ensure the ruler was perpendicular to the soil surface at all times.

Pasta may be broken by the anchor flukes' or axle, due to the relative sizes of these parts it is most likely that breakages were caused by the axle. All experiments yielded between 3 and 7 pasta samples which could be accurately measure ex-situ with a ruler to $+/-$ 0.5mm. To account for the uncertainty in failure all pasta depths and directly measured results are treated separately.

Shear strength measurements were taken with a shear vane and were precise to $+/-$ 0.1kPa.

The centrifuge speed is precise to $+/-$ 0.5rpm.

The experimental set-up is assumed to accurately represent the real world conditions, evidence for this is discussed in section 5 alongside the magnitude of maximum expected errors which are calculated in appendix I.

5 Results and discussion

All readings and observations are included in appendix II.

5.1 Experiment reports

As this experiment had never been carried out before, the first four of the nine experiments didn't produce results, but yielded valuable lessons which are summarised below in table 1.

Experiment	Date	Comments
1	05/12/13	• 80l Kaolin clay consoldated at 25g. • Pulley broke free of actuator and experiment stopped. • More clay required to get sufficient depth. • Styro-foam support initially required to support anchor as clay has insufficient strength at surface. • New pulley designed to be made of a single piece of material and fixed to the actuator by two grub screws. • Increase chain length on rode to 0.2m to ensure drag force acting on the anchor is parallel to soil surface. • Use dye on fluke tips of anchor and place spaghetti radially in clay to get more penetration depth measurements.
2	27/01/14	• 100l of Kaolin clay consolidated at 25g, sufficient clay volume. • Actuator had insufficient power to pull anchor more than a few cm in clay, most likely damaged in previous breakage, no test possible. • Every fifth link of anchor rode painted to make observation of anchor penetration with the strobe easier. • Gearbox on actuator replaced with higher ratio.
3	28/01/14	• 100l of Kaolin clay consolidated at 25g. • Standpipe system failed to control the water level, not possble to run experiment.

Experiment	Date	Comments
4	13/02/14	• 100l of Kaolin clay consolidated at 40g. • All visible consolidation had ceased after 1.5hrs, when the centrifuge started to slow all the clay fell out. • Upon excavation it was found that the bond between the clay and geomembrane layer was of insufficient strength. • New geo-membrane purchased with a more fibrous, rough texture to aid bonding.
5	20/02/14	• 100l of Kaolin consolidated at 40g. • Anchor rode (fishing line) snapped after being dragged 2/3rds of proposed route. Anchor sank and pierced the drainage material. • Pasta marked penetration depth very successfully. • Dye on anchor fluke tips did not leave a very obvious trail in the clay as hoped. • Some results obtained at 40g test speed.
6	04/03/14	• 120l Kaolin clay consolidated at 80g. • Anchor cable initially broke but was replaced. • Measurements taken at 40g test speed.
7	04/03/14	• 120l Kaolin clay consolidated at 80g. • Measurements taken at 20g test speed. • Anchor was seen to twist and flip over along its shaft axis during the experiment.

Experiment	Date	Comments
8	11/03/14	• 120l Kaolin clay consolidated at 40g. • Measurements taken at 20g test speed. • Anchor was seen to twist and flip over along its shaft axis during the experiment.
9	11/03/14	• 120l Kaolin clay consolidated at 40g. • Measurements taken at 10g test speed.

Table 1: Summary of experiments carried out

5.2 Soil profiles

5.2.1 Experimental soil profiles

For all experiments, shear vane readings taken at various depths into the consolidated clay give an undrained soil strength profile for the test soil. These have been plotted for the clay consolidated at 80g (experiments 6 & 7) and 40g (experiments 5, 8 and 9) and are shown in figure 16. All measurements are not scaled by the centrifuge test speed at this point but are as measured.

As can be seen from figure 16 the undrained soil strength profile produced by consolidating at an increased g level increases linearly with depth from the origin.

Two separate soil samples were consolidated at 40g, one used in experiment 5 and another used in experiments 8 & 9. When plotted separately they had lines of best fit $S_u = 32.5y$ and $S_u = 33.7y$ respectively. They therefore have a difference in gradient of 3.6 %, however the maximum expected error for this gradient is 7.7 % (full calculations in appendix I). It was therefore decided to use a single best fit line applied to all these data points. This has the equation $S_u = 33.4y$ corresponding to a model undrained shear strength gradient $K_{S_U} = 33.4kPa/m$.

Only a single soil sample was consolidated at 80g, readings from this sample give a line of best fit $S_u = 100y$ and corresponding model undrained shear strength gradient $K_{S_U} = 100.0kPa/m$.

Both lines of best fit are based on a large number of points and considering the maximum precision of the shear vane used is $+/-$ 0.1kPa, there is relatively small spread in the results, especially for the soil consolidated at 80g. Both lines of best fit are forced through the origin as these are normally consolidated clay samples and so there is zero shear strength at the surface by definition. Therefore it is concluded that the undrained shear strength increases linearly with depth from 0 at a rate of $K_{S_U} = 33.4kPa/m$ and $K_{S_U} = 100.0kPa/m$ for kaolin clay consolidated at 40g and 80g respectively.

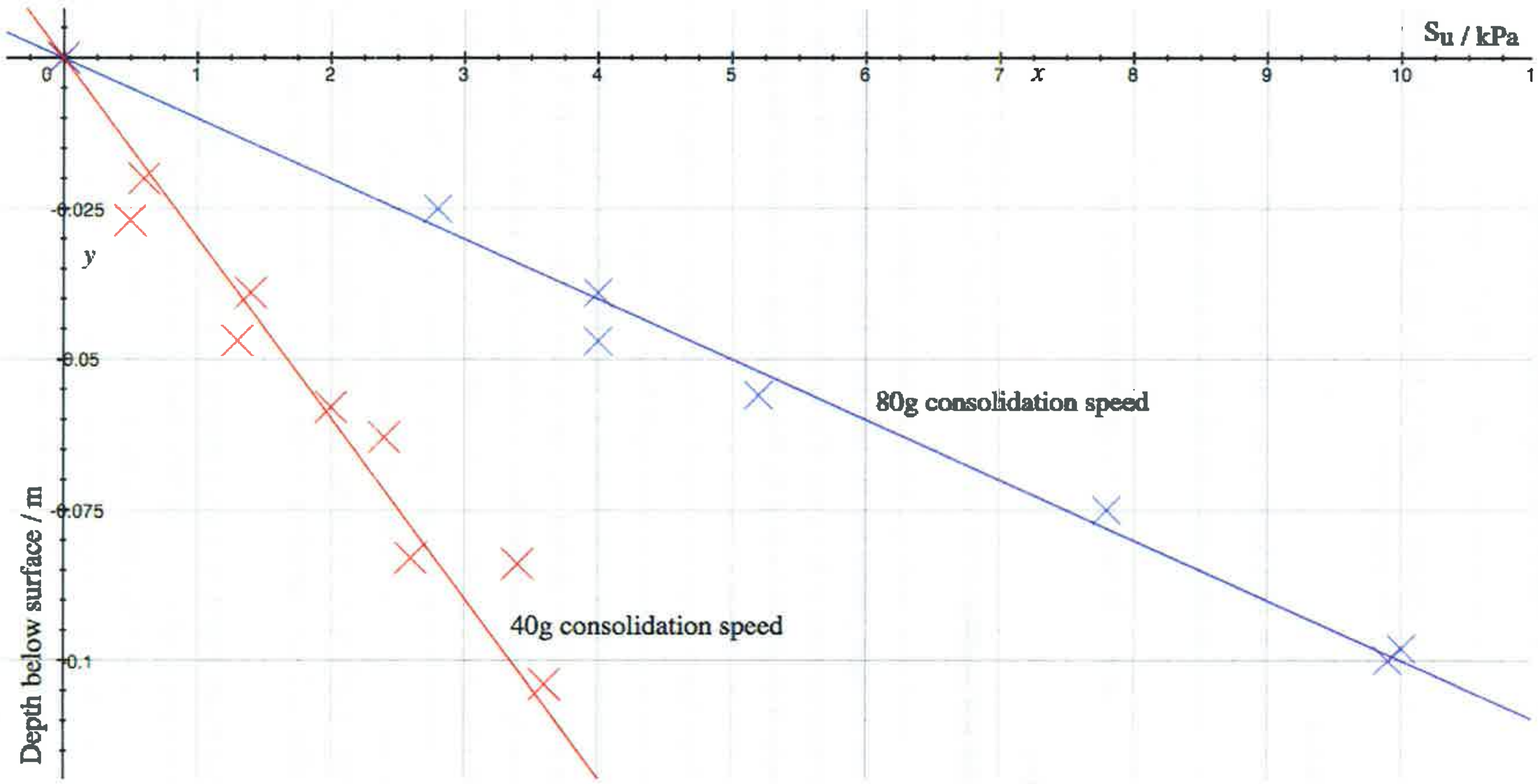

Figure 19: Graph of undrained shear strength against depth for Kaolin clay consolidated at 80g and 40g

5.2.2 Shear strength profiles of real seabeds

In-situ testing of the seabed is commonly carried out using penetrometer testing carried out from ROVs. Cone penetrometers have a small area ($10cm^2$), in soft subsea formations this leads to low tip resistances, making empirical correlations less accurate, in addition the deformation mechanism in the vertical plane is reported to be asymmetric resulting in additional correction of results being required to account for pore and overburden pressures. Therefore T-bar penetrometers are more commonly used; they have a much larger area and the soil flow around them is symmetrical meaning empirical correlations relate the bearing pressure to the undrained shear strength of the soil without need to account for the overburden [18].

Testing carried out by Newson et al. [18] measured the undrained shear strength profile of the clayey seabed of the Nile delta using standard cone penetrometer testing (CPT), enlarged head CPT and T-bar penetrometer testing as shown in figure 20. It was found that the undrained shear strength profile increased linearly from 0 at the surface at a rate of 1kPa per meter depth. This gives an equivalent strength relationship to Kaolin consolidated at 40g and tested at 33g. A similar test in Thistle field, North Sea, found the undrained shear strength profile increased linearly from approximately 0kPa at the surface at a rate of 13kPa/m [20], which could be replicated by soil consolidated at 80g and tested at 8g. In conclusion, the centrifuge modelling accurately replicates the seabed conditions.

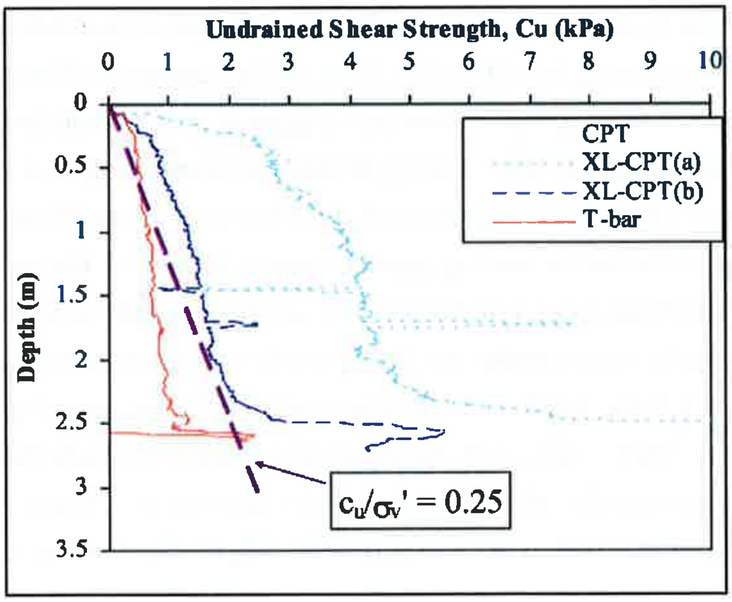

Figure 20: Graph of undrained shear strength profile from the Nile Delta [18]

5.3 Penetration readings

The average penetration depth for each test and the corresponding undrained shear strength is shown below in table 2.

Experiment	Model K_{S_U} kPa/m	Test speed / g	Final measured depth / mm	Prototype final depth / m	Undrained shear strength at final depth/ kPa
5	33.4	40	57	2.29	2.0
6	100.0	40	45	1.80	4.5
7	100.0	20	43	0.86	4.3
8	33.4	20	45	0.9	1.5
9	33.4	10	44	0.44	1.4

Table 2: Table of average penetration depths and undrained shear strengths for all tests

Table 2 shows that a 280kg anchor (corresponding to a 20g test speed) has a greater penetration depth of 2.29m in soil consolidated at 40g than the 1.80m penetration depth in soil consolidated at 80g. The same relationship is true for a 2240kg anchor (40g test speed) however the magnitude of the difference is only 0.04m compared to 0.36m for the 280kg anchor. The exact reasons for this behaviour are dependent on the exact scaling of the relative sizes and are discussed in section 5.3.2. However, with the findings in section 5.2 it is possible to conclude that soil consolidated at greater speeds has a larger undrained shear strength gradient and this means a comparable anchor will reach its equilibrium depth at a smaller penetration depth than in soil consolidated at a lower speed.

It is also interesting to note that corresponding anchors penetrate down to soil with much greater undrained shear strength in stiffer clay. Tests at 40g (corresponding to a 2240kg anchor) record a soil strength of 2.0kPa at equilibrium penetration in clay consolidated at 40g compared to 4.5kPa in clay consolidated at 80g. Testing at 20g (corresponding to a 280kg anchor) also produced this factor of 2 difference in undrained shear strength at equilibrium penetration.

Analysis of the results for increasing anchor masses in soil of the same strength shows that larger anchors penetrated the soil deeper and reached equilibrium at increasingly large undrained shear strengths, for example the 280kg anchor (20g test speed) penetrated 0.9m to soil with a strength of 1.5kPa, whereas the 2240kg anchor (40g test speed) penetrated 2.29m to soil with a strength of 2.0kPa. Although the exact relationship between these two variables is not evident from the raw results, this behaviour is as expected as a larger mass will require a stronger force to support it, which will be experienced deeper into the clay layer.

5.3.1 Anchor behaviour

Observation during testing showed that the anchor, initially situated in the first few centimeters of soil, would penetrate the soil more deeply as a horizontal force was applied. This increase in penetration occurred over about 100mm, after which the anchor progressed through the soil at a constant depth as clearly indicated in experiment 5. This experiment yielded three broken pasta samples equally spaced along the drag length with measured penetration depths of 45mm, 44mm and 43mm below the clay surface (see appendix II for raw data). Given the accuracy of measurement being at best $+/-$ 0.5mm it is suggested that the anchor finds an equilibrium depth at which it is dragged.

A physical explanation for this behaviour may be that the downward inclined flukes, interacting with the soil under the action of a horizontal force, exerts a vertical force downwards, pulling the anchor deeper into the soil. The anchor therefore penetrates deeper until this vertical component and the anchor's own weight are balanced in the vertical direction by the increased strength of the soil at greater depth. The anchor therefore finds and moves at an equilibrium depth where these forces are balanced. A mathematical model based on this concept is developed in section 5.3.3.

5.3.2 Dimensional analysis

This experiment has not been carried out before and there are many variables involved. Dimensional analysis is therefore used to both gain a better understanding of the physical problem and allow easier interpretation of the experimental results. The following variables are considered to be involved in the problem:

- Penetration depth - d $/m$
- Undrained shear strength gradient- K_{S_U} $/kPa/m$
- Anchor mass - M / kg
- Anchor density - ρ_s / kgm^{-3}
- Gravitational acceleration - g / ms^{-2}
- Anchor geometry, expressed as the shaft length - L / m

Dimensional analysis leads to the following relationship:

$$\frac{d}{L} = f[\frac{K_{S_U}L^3}{mg}, \frac{\rho_s L^3}{m}]$$

In the following the subscript p denotes a prototype value and the subscript m a model value. For the calculation of non-dimensional groups all scaling cancels and so any consistent set of model or prototype values can be used.

Both L_p and m_p are dependent on the test speed, S_u and d are measured directly from the experiment and ρ_s and g_p are constant. It is therefore planned to produce a graph of $\frac{d}{L}$ against $\frac{K_{S_U}L^3}{mg}$. $\frac{\rho_s L^3}{m}$ will be constant as the same model anchor is used in all experiments.

The calculated non-dimensional groups for each experiment are shown in table 3. L_m is taken as 0.064m, the shaft length of the model Danforth anchor at 1g, which is then scaled according to the test acceleration. $\frac{\rho_s L^3}{m}$ = 19.47 for all experiments based on a steel density of 2600 kgm^{-3}.

These results are shown graphically in figure 21.

Experiment	Consolidation speed / g	Test speed / g	$\frac{d}{L}$	$\frac{K_{S_U} L^3}{mg}$
5	40	40	0.89	0.64
6	80	40	0.70	1.91
7	80	20	0.67	3.82
8	40	20	0.70	1.28
9	40	10	0.69	2.55

Table 3: Table of non-dimensional groups

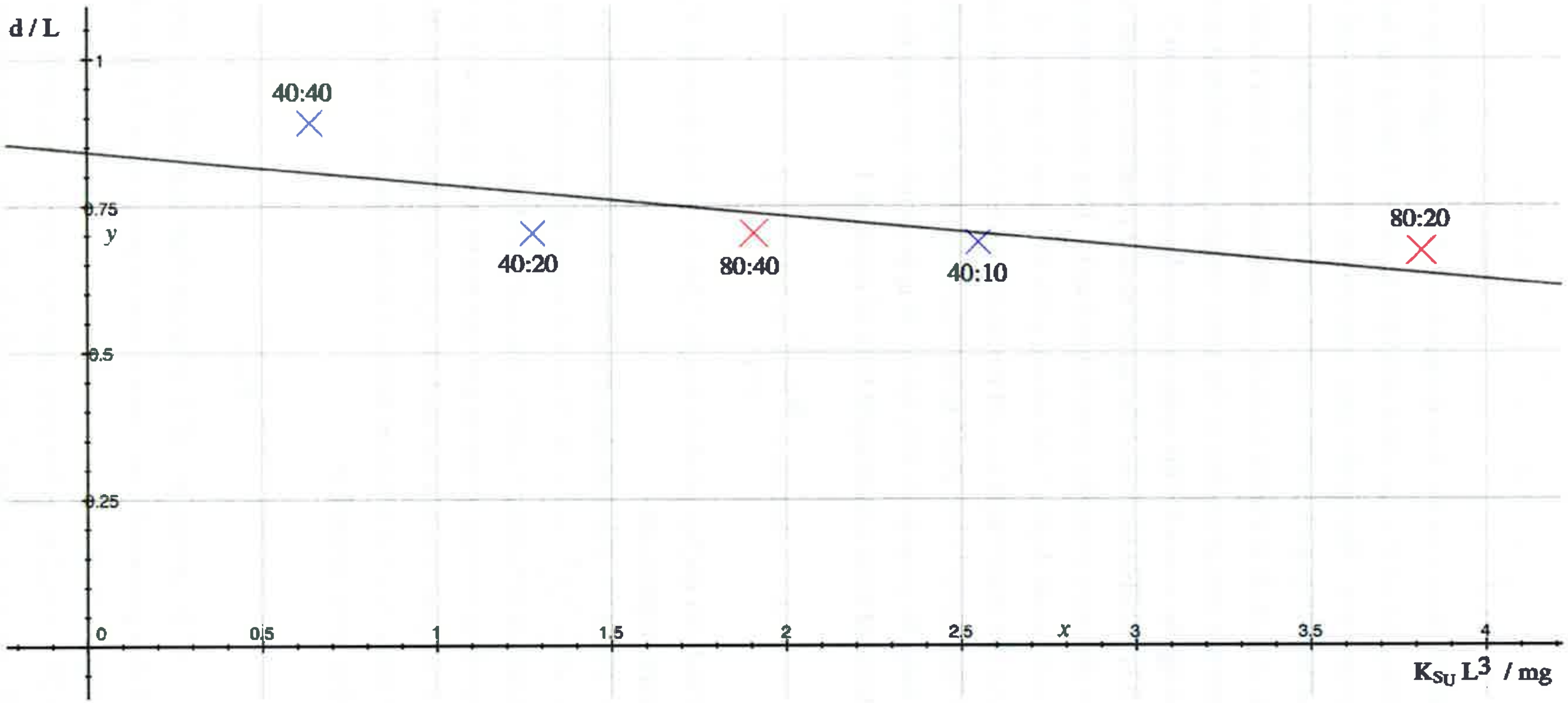

Figure 21: Graph of dimensionless penetration depth against dimensionless soil strength; [consolidation acceleration(g):test acceleration(g)]

Figure 21 shows that $\frac{d}{L}$ decreases with an increasing $\frac{K_{S_U} L^3}{mg}$ according to the equation:

$$\frac{d}{L} = -0.0545 \times \frac{K_{S_U} L^3}{mg} + 0.8422 \tag{1}$$

The penetration depth decreases as the non-dimensional shear strength mass ratio increases, either through increasing the undrained shear strength gradient, making the soil stronger and / or reducing the anchor mass. Physically this corresponds to a stronger soil being better at resisting the weight of a smaller anchor which agrees with the above model.

As a result of this, the smallest anchor for each consolidation speed is located further along the x-axis than the heaviest and an anchor of the same weight, consolidated at a greater speed will also be further along the x-axis for the same reasons discussed in section 5.

From equation 1 it is possible to predict the upper bound penetration depth of various sizes of Danforth anchor in different normally consolidated soils. This maximum penetration depth equals the minimum safe burial depth of the subsea cable that is to be protected.

Once the mass (m_p) and shaft length (L_p) of the largest anchor that a cable must be protected from has been established, an accurate prediction of the undrained shear strength gradient K_{S_U} must be established along the proposed cable route. At appropriate spacings the required burial depth can then be calculated from a rearranged form of equation 1:

$$d = -0.0545 \times \frac{K_{S_U} L^4}{mg} + 0.8422 \times L \tag{2}$$

Based on a 2000kg Danforth anchor of shaft length 2.5m in soil of strength K_{S_U} = 10kPa/m, the predicted penetration depth is 2m.

As can be seen in figure 21, this correlation predicts that the non-dimensional penetration depth will equal zero when $\frac{K_{S_U} L^3}{mg} = 15.45$. This will occur if excessively large shear strength gradients are used, based on the above example, this occurs when $K_{S_U} = 19.4kPa/m$. This is a very large undrained shear strength gradient and will not be met in any soft clay.

One of the main assumptions is that the anchors scale according to the shaft length. This is largely true, however there is some variation between manufacturers. The expected value of L is $L_E = 0.064Nm$ where N is defined as:

$$N = \sqrt[3]{\frac{m_p}{0.035}} \tag{3}$$

Where m_p is the mass of the prototype. If L is larger than expected the area of the anchor is likely to be greater than predicted above and a smaller penetration depth will result, if L is smaller, penetration may be deeper.

The line in figure 21 is based upon 5 points, although there is reasonably small spread, it is clear that if the 40:40 point was excluded there would be an even smaller spread and the line of best fit would be approximately horizontal. This result would occur if the apparatus incorrectly modelled real world behaviour and restrained the anchor so that it was forced to move at a constant depth and angle. Visual observation found that the angle of the anchor during motion changed over the first 10cm before moving with the flukes parallel to the surface of the clay. Similarly inspection of table 2 suggests the anchor may have been restrained as all measured penetration depths are very similar. However this table does not account for the difference in depth of the clay surface, this level varied from 87mm below the channel in experiment 7 to 41mm below the channel in experiment 8. Therefore the anchor has complete freedom of movement within the apparatus and this analysis is not valid. Additionally, there is little experimental evidence for data point 40:40 on figure 21 being anomalous however a repeat experiment would be desirable.

If the undrained shear strength profile was not of the form $S_U = K_{S_U} z$, where z is the depth below the soil surface, but instead varied as $S_U = K_{S_U} z + S_{U0}$ it would also be possible to predict the penetration depth. Using the original procedure detailed above, a value of d_1 would be found from equation 2 using the anchor mass (m_p), shaft length (L_p) and undrained shear strength gradient K_{S_U} . The value of undrained shear strength would then be calculated using $S_{U1} = K_{S_U} d_1$, by substitution into the equation for soil strength in that soil the actual penetration depth (d_2) can be established: $K_{S_U} d_1 = K_{S_U} d_2 + S_{U0}$.

5.3.3 Mathematical modelling of anchor penetration

Both numerical and analytical methods have been used to model the behaviour of drag anchor. These methods calculate the soil pressures exerted on the anchor using bearing-calculations before incrementally advancing the anchor along the calculated embedment path, using moment equilibrium to determine the new direction of the anchor and assuming the anchor travels parallel to the fluke direction. An example is shown in figure 22.

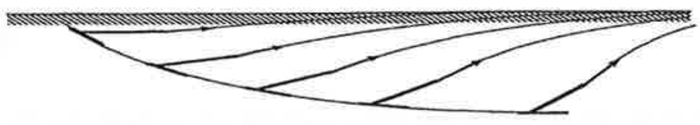

Figure 22: Anchor embedment trajectory [21]

All the previous work encountered deals with drag anchors, a type of large scale mooring anchor that is intentionally dragged along the seabed for a period of time to embed it below the surface, increasing its maximum holding capacity. Although much larger, there are many geometric similarities between drag and Danforth anchors as shown in figures 23 and 13 respectively. Both anchors rely on their flukes to increase embedment, the angle between the fluke and shanks, although variable, is in the same range and both can be dragged behind a vessel. This section therefore outlines the existing results for embedment of drag anchors, produces a Danforth specific model and compares the results to experimental findings.

Figure 23: Picture of a drag anchor [22]

Initially the anchor is positioned with the flukes at an angle to the soil surface as would be expected if the anchor reached the seabed under gravity, they therefore embed and the forces acting on the anchor are as shown in figure 24. Near the surface the weight is much greater than the resultant force due to the soil resistance, as a result there is a resultant anti-clockwise moment acting on the anchor, this causes it to rotate. Additionally, the vertical downward forces at this point far exceed the vertical upward forces and so the anchor penetrates deeper into the soil.

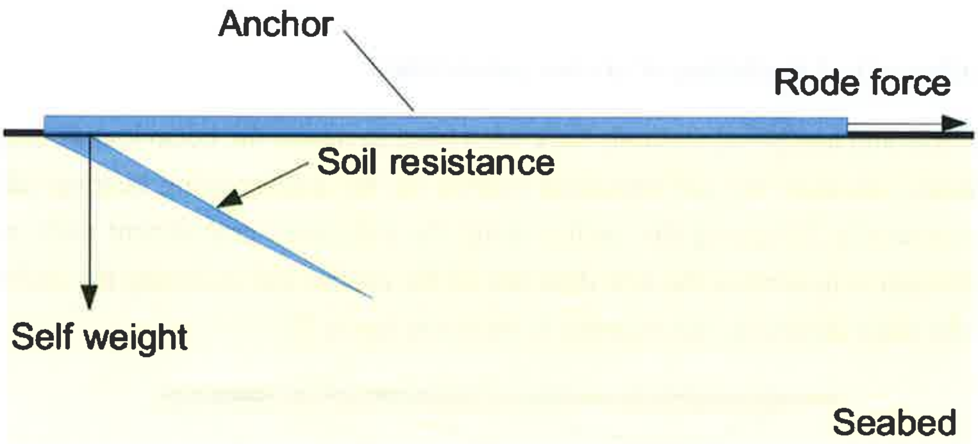

Figure 24: Simplistic diagram showing the forces acting on a Danforth anchor as it penetrates the surface

The assumption that drag anchors travel in the direction parallel to their flukes is commonly accepted and has been established through observation, modelling [21] and field tests [24]. It is therefore considered an appropriate assumption for a Danforth anchor. Therefore, once the anchor has reached its maximum penetration depth, the flukes are horizontal. Assuming the anchor moves sufficiently fast that undrained conditions can be assumed but slow enough so that inertial affects can also be neglected, a force diagram can now be assumed as in figure 25.

Additionally it is assumed that:

- The anchor shaft has negligible depth in the plane of the page (based on figure 25).

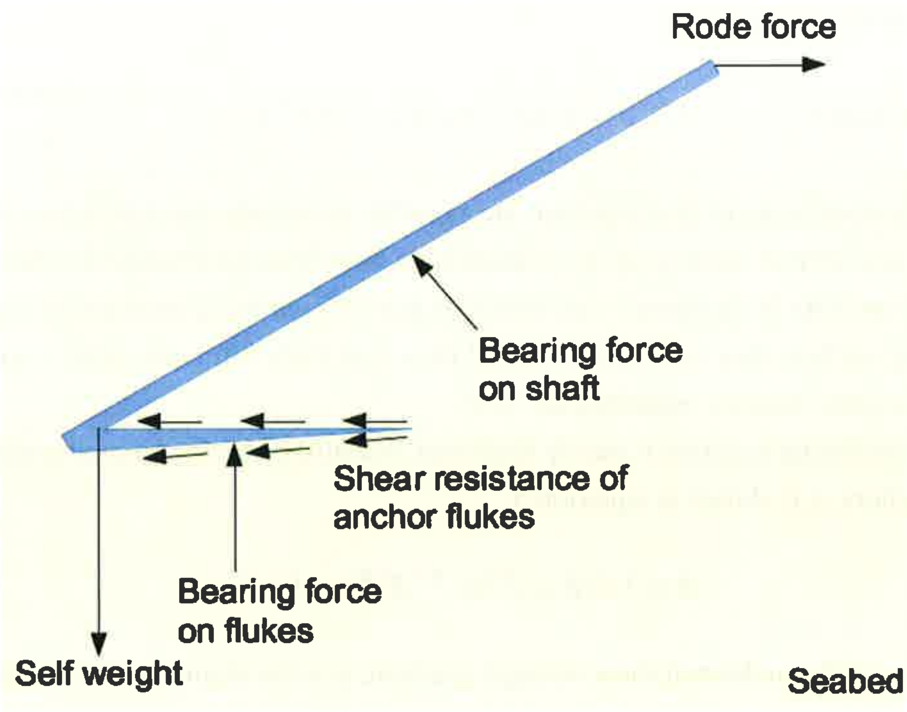

Figure 25: Simplistic diagram showing the forces acting on a Danforth anchor as it penetrates the surface

- The fluke tip has negligible area.
- Interactions between the anchor and soil can be modelled as bearing failures.

Vertical equilibrium implies that the self weight ($m_p g$) is balanced by the reaction of the soil acting upon the flukes (F_f) and shaft (F_s):

$$F_f + F_s = m_p g_p$$

As the anchor is being pulled horizontally, the horizontal projected area of the shaft equals:

$$0.004 \times 0.064 sin(60) N^2 (m^2)$$

This area experiences a soil resistance of $(2+\pi)S_U$ in N/m^2, if it is assumed that the fluke depth is d, using the undrained shear strength gradient results in a horizontal force exerted on the shaft given by:

$$F_s = 0.000128\sqrt{3}(2+\pi)N^2 K_{S_U}(\frac{d+(d-0.064N sin(60))}{2} \text{ N}$$

Similarly the area of the flukes is $0.0005694N^2m^2$, using the same approach as above gives a fluke force:

$$F_f = 0.0005694N^2(2+\pi)k_{S_U} d \text{ N}$$

Overall this yields the equation:

$$m_p g = 0.0005694N^2(2+\pi)K_{S_U}d + 0.000128\sqrt{3}(2+\pi)N^2K_{S_U}(\frac{d+(d-0.064Nsin(60)}{2}) \tag{4}$$

Further developments of this equation are possible to include the interaction of the chain with the soil and several more complex relationships have been established for the embedment depth of drag anchors in undrained clay, however due to the limited similarities between Danforth and drag anchors they have been omitted from this study until any direct correlation can be shown. For more detailed equations see [12].

Another interesting equation is purely empirical, established by the Vryhof company for use with drag anchors, it is shown in equation 5.

$$d = 1.5(K_{S_U})^{0.6}\psi^{-0.7}A^{0.3}(tan\theta_s)^{1.7} \tag{5}$$

Where K_{S_U} is the undrained shear strength gradient, ψ is the diameter of the embedded drag lines, A is the fluke area and θ_s is the shank-fluke angle [12].

Figure 26 shows the empirically and mathematically predicted penetration depths (equations 4 and 5 respectively) superimposed upon the experimental results (equation 2).

Figure 26 shows the results of applying the empirical drag anchor equation (blue) to Danforth anchors. It firstly overestimates the penetration depth greatly and results in a decreasing penetration depth as the anchor mass increases. This does not agree with any of the other results found. Inspection of equation 5 shows that it is very dependent on ψ, the chain diameter. Conventional drag anchors have several meters of their rode buried in the clay, conversely the Danforth anchor was seen with a maximum of three links of it's rode submerged. The chain is therefore likely to have much less impact on a Danforth anchor and therefore a power more like -0.9 would maybe be better. Similarly, drag anchors have a much greater surface area than Danforth anchors, therefore it is also likely that an empirical equation for the embedment of a Danforth anchor would have even less emphasis placed on the area.

The mathematical model (red), based on principles used for modelling drag anchors, yields a better fit. The model correctly shows the anchor penetration depth increasing linearly with anchor mass from the origin. However it does overestimate the penetration in soft clay and underestimate penetration in harder clay. This may be due to any of the simplifying assumptions above however the simplified model is a good initial estimate.

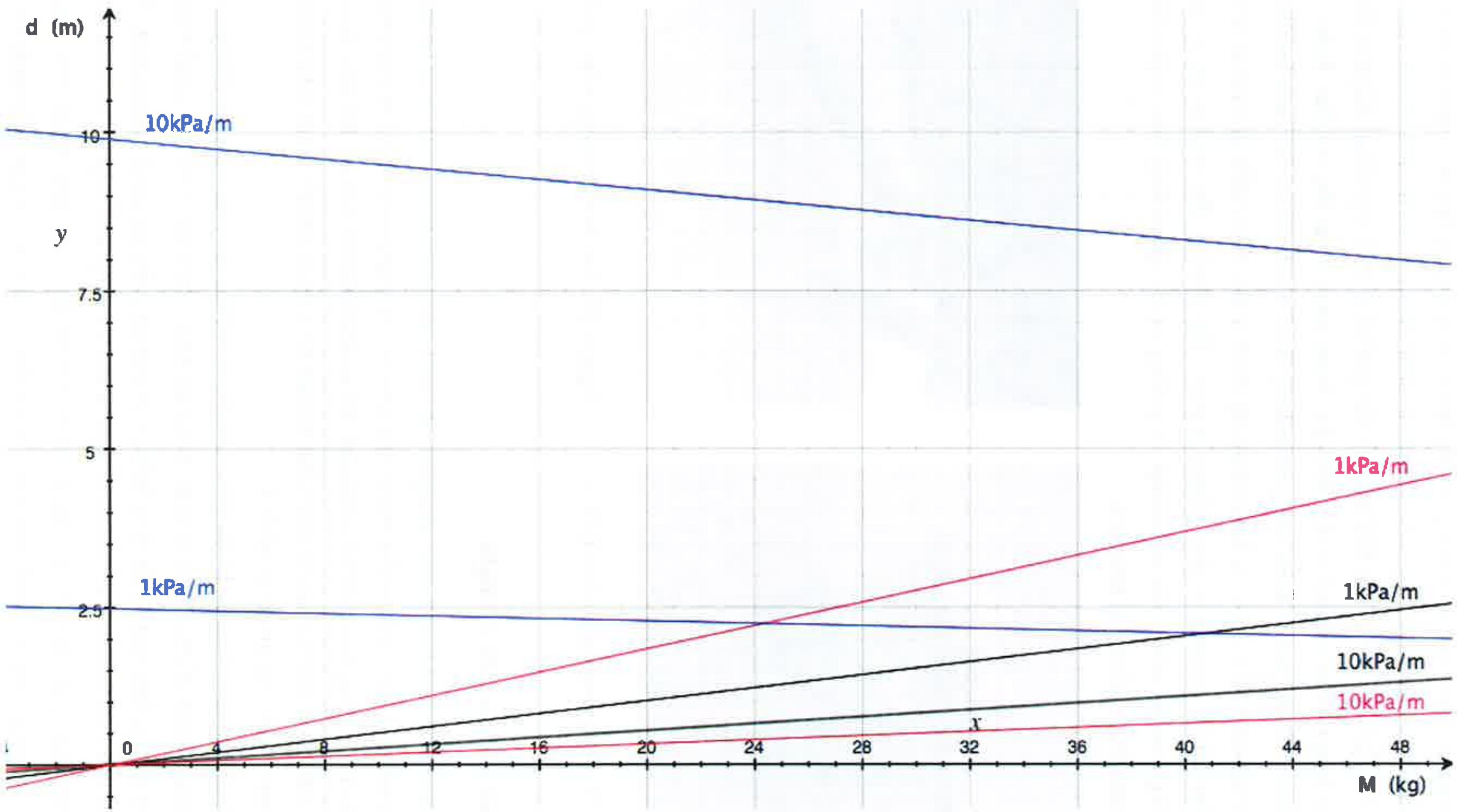

Figure 26: Graph of penetration depth against anchor mass for using empirical (blue), mathematical (red) and experimental (black) results

5.3.4 Anchor twisting

During experiments 7 and 8, both testing at 20g test speed, the anchor was seen to rotate about the axis of its shaft. Close visual inspection of the anchor showed that the flukes were not exactly the same size (figure 27) and when this anchor was pulled across styrofoam (figure 28) it was found that the larger fluke tended to dig into the foam more than the smaller fluke, making the anchor rotate. These small flaws are particularly hard to eliminate in such small models. The fact that rotation didn't occur in the remaining three trials, especially at a lower test speed, implies that the initial placement also played a part. By placing the anchor on a styrofoam support at a slight angle whilst the centrifuge is getting up to speed may have exacerbated the physical differences, resulting in rotation.

Figure 27: Asymmetric anchor flukes

Figure 28: Anchor twisting when pulled

5.3.5 Anchor rode tensile strength

During experiments 5 and 6, the rode snapped. In both cases this break occurred in the fishing line. In experiment 5 this occurred towards the end of the experiment and in experiment 6 it occurred at the beginning so could be replaced. To understand the reason for this, tensile tests of the fishing line were carried out by applying weight to a small sample until it failed as shown in figure 29, the results are given in table 4.

The nominal breaking load is 15lbs (66.71N) however the average recorded force at failure was 57.16N. Inspection of the above results shows a consistently lower failure load than quoted. One reason for this is that four of the five failures occurred at the point of connection. To create a loop, both in this experiment and during testing, a small crimp was applied as shown in figure 30, this caused small dents in the wire, these areas of weakness therefore broke first. Due to this trend and the fact that breakage only occurred twice during testing, it can be concluded that the wire broke at points of weakness caused by abrasion or mechanical wear and at no point did the test a horizontal force in excess of 57.16N on the anchor.

Sample	Failure load / N
1	56.54
2	57.63
3	56.70
4	57.29
5	57.62

Table 4: Table of measured failure loads

Figure 29: Picture of the experimental setup

Figure 30: Crimp connecting fishing wire

5.3.6 Static and dynamic penetration depth comparison

Using shallow foundation theory the undrained bearing capacity of the test soil was used to estimate the static penetration depth that would be achieved by releasing an anchor on the seabed. The maximum depth was predicted using equation 6:

$$V_{max} = q_f A = A \times ((2+\pi)d_c S_U + \gamma_s h) \tag{6}$$

The soil is assumed undrained and to have undrained shear strength profiles as in section 5.1. Using equation 6 and assuming:

- A = $0.0005694m^2 \times N^2$, where N is found from equation 3.
- $S_u = k_{S_U} h$ where h is the penetration depth and k_{S_U} is as calculated in section 5.1.
- γ_s is assumed to equal $20kPa/m^3$.
- The embedment factor is taken as $d_c = 1 + 0.33tan^{-1}(h/0.0005694N)$

Values of V_{max} are calculated at 0.1m increments of h for each of the two values of K_{S_U} given and for N = 10, 20 and 40. By comparing the resultant resistances (table 5) to the weight of the anchor at 10g, 20g and 40g (table 6), the predicted embedment depth is obtained.

k_{S_u}	100 kPa/m		33.4 kPa/m		
Anchor mass / kg	280	2240	35	280	2240
h / m	V_{max}				
0.1	1.32	3.51	0.26	0.75	2.39
0.2	2.67	7.11	0.52	1.50	4.80
0.3	4.01	10.71	0.79	2.25	7.22
0.4	5.36	14.31	1.05	3.00	9.63
0.5	6.70	17.91	1.31	3.75	12.05
0.6	8.05	21.51	1.57	4.51	14.47
0.7	9.39	25.11	1.83	5.26	16.88
0.8	10.73	28.71	2.10	6.01	19.30
0.9	12.08	32.31	2.36	6.76	21.71
1.0	13.42	35.91	2.62	7.52	24.13

Table 5: Table of maximum undrained vertical capacity against depth of penetration for given soil strength gradients and anchor masses

N	Anchor weight / kN
10	0.34
20	2.75
30	9.27
40	21.97
50	42.92

Table 6: Table of anchor weights and corresponding gravitational accelerations

Due to the limited accuracy of the measured dynamic penetration depths, the predicted static penetration depths are only calculated to the nearest 0.1m. The calculated values are given in table 7.

Experiment	Anchor Mass / kg	$K_{S_u model}$ / $kPam^{-1}$	Predicted static penetration depth / m	Measured dynamic penetration depth / m
5	2240	33.4	0.9	2.3
6	2240	100.0	0.6	1.8
7	280	100.0	0.2	0.86
8	280	33.4	0.3	0.9
9	35	33.4	0.1	0.4

Table 7: Table of predicted static and measured dynamic penetration depths

These calculated depths are most likely an overestimate as they do not account for the movement of clay around the anchor as it sinks.

Comparing the measured dynamic penetration depth to the static predicted depth shows that the horizontal force acting on the anchor results in an increased depth by approximately a factor of 3. The horizontal force attempts to pull the anchor through the clay, but the downward angle of the flukes being resisted by the soil results in a vertical force downwards, pulling the anchor deeper. The anchor is therefore pulled through the soil at a new equilibrium depth where its weight and the vertical force created by the fluke interaction with the soil are balanced by the soil resistance as shown in section 5.3.3.

5.4 Future experimentation

This project has developed an experimental apparatus and method that has been proven to give valuable results. However there are several ways in which this could be further improved in future:

- Develop a new method of attaching the fishing wire to the anchor chain to reduce the number of breakages. It may be better to replace the fishing wire with metal wire for added strength.
- Produce a more accurate anchor and build a specialist support stand that ensures the anchor axle is parallel to the clay surface to prevent rotation during testing.
- Collect data over a greater range of anchor masses (varying the test acceleration from 10g to 100g) and over a greater range of soil strength profiles. This will produce more data points and make the resultant design line more reliable.
- Collect data with different types of anchor, in particular exploring Hall and HHP APC 14 anchors which have repeatedly come up during reading around the subject.
- Develop better methods of measuring the undrained shear strength. Due to the lack of homogeneity, shear strength samples cannot be removed from the centrifuge for testing and so triaxial, direct shear and fall cone testing is not possible. The most effective way to increase the accuracy of the shear strength measurements is to obtain a shear vane with a larger head, calibrated for use in softer soils.
- Carry out tests in sand samples. This poses significant challenges in the drum centrifuge as it cannot be stopped to swap the spreader for the test equipment as all the sand will fall out. A single piece of apparatus combing both items would therefore be required.

6 Conclusions

In conclusion, centrifuge testing enables accurate representation of anchor dragging in soft clay soils. Consolidation of clay at different centrifuge speeds produces a linearly increasing undrained strength profile comparable to that found in the seabed. By consolidating at higher speeds larger gradients can be produced. Experiments showed that an anchor dragged through these soils establishes an equilibrium depth traveling in a direction parallel to the flukes and a relationship between the undrained shear strength gradient, anchor size and penetration depth was established.

The relationship given in equation 1 allows safe burial depths for subsea cables to be calculated to protect them from damage by anchors being dragged behind ships. This is a conservative design line however it enables more effective burial than using net burial depths. This can lead to cost and emissions savings over the whole life of the project making cable burial more sustainable. Based on this line, the burial protection index (BPI), figure 2, [10] is overly conservative. To establish BPI 2 (protection against anchors up to 2 tonnes) in very soft clays it is implied that burial to 5m depth is required. Assuming a clay of strength 1kPa/m, the design line derived here recommends a burial depth of 1.97m. This agrees with the findings of experiments by the German Coastal Department [11], their trials in fine sand in German Bight produced measured penetration depths a factor of 2 smaller than predicted by BPI. The alternative design chart in figure 31 is therefore suggested. This chart has a safety factor of 2 for anchors of 100kg reducing to a factor of safety of 1 for anchors of 4000kg, reflecting the decreasing probability of larger anchors accidentally being deployed in the area as the design anchor mass increases.

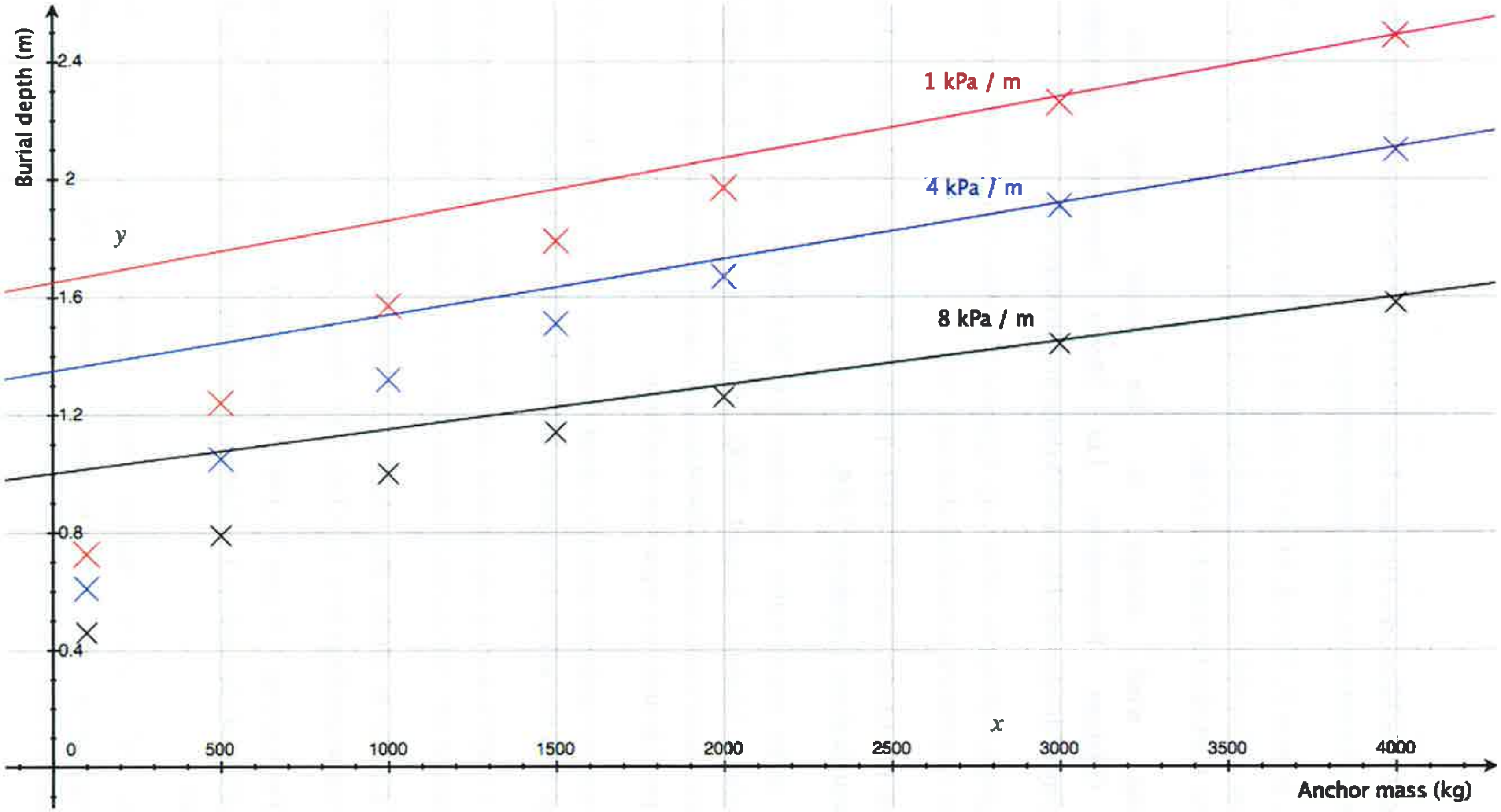

Figure 31: Proposed design chart for determining safe cable burial depth in soft clays, predicted penetration depths marked with crosses

7 Bibliography

References

[1] Submarne Cable Networks. Updated June 2011; Cited December 2013. Available from: http://submarinenetworks.com/systems/categories

[2] Carter L, Burnett D, Drew S, Marle G, Hagadorn L, Bartlett-McNeil D, Irvine N. (2009) Submarine cables and the oceans: connecting the world. UNEP-WCMC Biodiversity Series No.32. ICPC/UNEP/UNEP-WCMC.

[3] Developing wind energy in the outer Moray Firth. (2012) Moray Offshore Renewables Ltd Media Summary. Available from: http://morayoffshorerenewables.com/Documents/Brochure.aspx

[4] TeleGeography submarine cable map. Updated November 2013; Cited May 2014. Available from: http://www.submarinecablemap.com

[5] Shapiro S, Kordahi M, Lucas G. (2006) Trends in Submarine Cable System Faults. Tyco Telecommunications. Eatontown. USA.

[6] Atlantic cable maintenance agreement (ACMA 2001) to provide undersea repair services. Updated August 2000; Cited December 2013. Available from: http://www.sourcewire.com/news/8464/atlantic-cable-maintenance-agreement-acma-2001-to-provide-undersea-repair-services?hilite

[7] 2008 submarine cable disruption. Updated December 2013; Cited December 2013. Available from: http://en.wikipedia.org/wiki/ 2008_submarine_cable_disruption

[8] Allan P. (1999) Selecting appropriate cable burial depths - a methodology. Conference Proceedings of IBC Submarine Communications 1999. Cannes. France. November.

[9] Allan P, Comrie R. (2001) The selection of appropriate burial tools and burial depths. Conference proceedings from SubOptic 2001. Kyoto. May.

[10] Mole P, Featherstone J, Winter S. (1997) Cable protection - solutions through new installation and burial approaches. Conference proceedings of SubOptic 1997. San Francisco. USA. May.

[11] Maushake C. (2013) Anchor tests German Bight. Federal Waterways and Engineering Research Institute. Hamburg. Germany. Available from: http://www.innomar.com/wssa2013/2013-wssa-Maushake.pdf

[12] Haixiao L, Ying L, Hanting Y, Wei Z, Chenglin L. (2010) Analytical study on the utimate embedment depth of drag anchors. Ocean Engineering. Vol 37. Issues 14-1. Pg 1292-1306.

[13] Lloyds Register of Shipping: Rules and Regulations for the Classification of Ships.

[14] Different types of anchor. Cited May 2014. Available from: http://www.infovisual.info/05/075_en.html

[15] West Marine: How to anchor securely. Cited May 2014. Available from: http://www.westmarine.com/WestAdvisor/How-To-Anchor-Securely

[16] Danforth Anchors. Updated October 2012; Cited December 2013. Available from: http://www.saxtonmarine.co.uk/danforth_anchor.html

[17] 4Coffshore: Equipment used. Updated January 2012; Cited May 2014. Available from: http://www.4coffshore.com/windfarms/about/equipmentTypes.aspx

[18] Newson T, Bransby M, Brunning P, Morrow D. (2004) Determination of undrained shear strength parameters for buried pipeline stability in deltaic soft clays. Paper number 04-JSC-266.University of Dundee. Scotland.

[19] Craig W, Taylor R, Phillips R, Powrie W, Kusakabe O. (1995) Geotechnical centrifuge technology. First edition. Chapman and Hall. London. pg 19-33.

[20] Wood D. (1990) Soil behaviour and critical state soil mechanics. Cambridge University Press. Cambridge. UK.

[21] Neubecker S, Randolph M. (1996) The performance of drag anchor and chain systems in cohessive soil. Marine Geosources and Geotechnology. 14:2, 77-96.

[22] Vryhof Anchors. Picture of Stevpris Mk6. Cited May 2014. Available from: http://www.vryhof.com/products/anchors/stevpris$_m$k6.html

[23] UK Yacht Rigging and Supplies. Image of a Danforth anchor. Cited May 2014. Available from: http://www.ebay.co.uk/bhp/10kg-anchor

[24] Vryhof Anchor Manual. (2005) Krimpen and Yssel. The Netherlands.

8 Appendix I

8.1 Calculation of error

To establish the error in the non-dimensional graph, the percentage errors are calculated for all quantities concerned. Where there is no obvious quantity with which to divide the instrument precision by and thus determine the relative error, the most critical value is used so as to give the largest realistic error.

- L - defined as the shaft length, scales with the centrifuge speed. The precision of the centrifuge speed is $+/-$ 0.5 rpm ($+/-0.79ms^{-2}, +/-0.08g$), L is therefore accurate to 0.79m, the smallest measurement was 10g therefore the relative error is $\frac{0.08}{10} = 0.008$.

- d - defined as the penetration depth, is accurate to $+/-$ 0.5mm, the smallest measured penetration depth is 3.9mm, the relative error is therefore 0.01. This is scaled by the test speed as it is a measure of depth for a given strength profile. The relative error of the smallest consolidation speed, 40g, is therefore $\frac{0.08}{40} = 0.002$, the relative error of d is therefore 0.012.

- S_u - defined as the undrained shear strength, is accurate to $\frac{0.1}{1.45} = 0.069$ based on the smallest reading of 1.45kPa and a precision of $+/-$ 0.1kPa.

- M - defined as the anchor mass, is accurate to 0.035kg $+/-$ 0.0005kg (0.014), this is also dependent on the centrifuge speed to the power of three. The total error is therefore: $0.014 + 0.008 + 0.008 + 0.008 = 0.038$

- The overall error for $\frac{d}{L}$ is the sum of the relative errors of each component quantity = $0.01 + 0.008 = 0.018(1.8\%)$.

- The overall error for $\frac{S_u L^2}{mg}$ is the sum of the relative errors of each component quantity = $0.069 + 0.008 + 0.008 + 0.038 = 0.123(12.3\%)$.

9 Appendix II

9.1 Experiment 5 observations and readings

Consolidation speed: 299rpm (40g)

Consolidation time: 2hrs2mins

Test speed: 299rpm (40g)

Depth of soil from channel top: 43mm

Calculated shear stress calculated from soil strength profiles shown in section 5.1 which are formed from the measured soil strength values.

Sample	Depth below clay surface / cm	Measured shear stress / kPa	Calculated shear stress / kPa	Comments
1	0	0	-	Soil profile
2	2.7	0.5	-	Soil profile
3	4.7	1.3	-	Soil profile
4	6.3	2.4	-	Soil profile
5	8.4	3.4	-	Soil profile
6	10.4	3.6	-	Soil profile
7	8.3	-	2.99	1st pasta break depth
8	5	-	1.70	2nd pasta break depth
9	4	-	1.32	3rd pasta break depth
10	5.6	-	1.94	Depth of anchor trail
11	4.3	-	1.43	4th pasta break depth
12	7.2	-	2.56	5th pasta break depth
13	4.4	-	1.47	6th pasta break depth
14	6.2	-	2.17	7th pasta break depth
15	6.1	-	2.13	8th pasta break depth

Table 8: Table of experimental observations and readings, experiment 5

Anchor rode broke (fishing line) after progressing around 2/3rds of planned route. Without horizontal force being applied the anchor sank to the bottom of the channel and pierces the drainage layer. As the failure occured after breaking the pasta, all penetration depth readings are considered accurate.

Average penetration depth: 57.3mm

Average undrained shear strength at penetration depth: 1.99kPa

9.2 Experiment 6 observations and readings

Consolidation speed: 423rpm (80g)
Consolidation time: 2hrs55min
Test speed: 299rpm (40g)
Depth of soil from channel top: 87mm

Calculated shear stress calculated from soil strength profiles shown in section 5.1 which are formed from the measured soil strength values.

Sample	Depth below clay surface / cm	Measured shear stress / kPa	Calculated shear stress / kPa	Comments
1	0	0.2	-	Soil profile
2	2.5	2.8	-	Soil profile
3	4.7	4	-	Soil profile
4	5.6	5.2	-	Soil profile
5	7.5	7.8	-	Soil profile
6	9.9	10	-	Soil profile
7	3.1	-	3.08	Depth to anchor axle
8	3.6	-	3.58	Depth to anchor axle
9	4.3	-	4.27	Depth to fluke tip
10	5.1	-	5.07	Depth to fluke tip
11	6.4	-	6.35	Pasta break depth

Table 9: Table of experimental observations and readings, experiment 6

Anchor rode broke (fishing line) at first attempt, anchor had not progressed so fishing wire was replaced and anchor completed it's traverse on the second run.

Average penetration depth: 44.7mm
Average undrained shear strength at penetration depth: 4.47kPa

9.3 Experiment 7 observations and readings

Consolidation speed: 423rpm (80g)
Test speed: 212rpm (20g)
Depth of soil from channel top: 87mm
Calculated shear stress calculated from soil strength profiles shown in section 5.1 which are formed from the measured soil strength values.

Sample	Depth below clay surface / cm	Measured shear stress / kPa	Calculated shear stress / kPa	Comments
1	0	0.2	-	Soil profile
2	2.5	2.8	-	Soil profile
3	4.7	4	-	Soil profile
4	5.6	5.2	-	Soil profile
5	7.5	7.8	-	Soil profile
6	9.9	10	-	Soil profile
7	3.9	4	-	Soil profile
8	5.2	7.6	-	Soil profile
9	9.8	10	-	Soil profile
10	3.7	-	3.68	Depth of fluke tip
11	4.4	-	4.37	Depth on anchor axle
12	4.9	-	4.87	Depth of fluke tip

Table 10: Table of experimental observations and readings, experiment 7

Anchor twisted along the axis of it's shaft, resulting in the flukes facing inwards. This occured half way along it's traverse as shown in figure 32. All pasta was forced out of the way in the wake of the twisted anchor and no reliable results could be obtained this way. All results obtained from its final position.

Average penetration depth: 43.3mm
Average undrained shear strength at penetration depth: 4.31kPa

Figure 32: Image of twisted anchor following 80g:20g test

9.4 Experiment 8 observations and readings

Consolidation speed: 299rpm (40g)

Consolidation time: 2hrs50mins Test speed: 212rpm (20g)

Depth of soil from channel top: 41mm

Calculated shear stress calculated from soil strength profiles shown in section 5.1 which are formed from the measured soil strength values.

Sample	Depth below clay surface / cm	Measured shear stress / kPa	Calculated shear stress / kPa	Comments
1	0	0	-	Soil profile
2	2	0.6	-	Soil profile
3	3.9	1.4	-	Soil profile
4	5.8	2	-	Soil profile
5	8.3	2.6	-	Soil profile
6	3.5	-	1.16	Depth to fluke tip
7	4.1	-	1.35	Depth to fluke tip
8	4.8	-	1.58	Depth to fluke tip
9	3.7	-	1.22	1st Pasta break depth
10	4.2	-	1.38	2nd Pasta break depth
11	4.6	-	1.51	3rd Pasta break depth
12	6.6	-	2.16	4th Pasta break depth

Table 11: Table of experimental observations and readings, experiment 8

As in experiment 7, the anchor was seen to twist about its shaft axis about one third of the way along its traverse. This experiment did however produce pasta breaks yielding more depth measurements.

Average penetration depth: 45.0mm

Average undrained shear strength at penetration depth: 1.48kPa

9.5 Experiment 9 observations and readings

Consolidation speed: 299rpm (40g)
Test speed: 149rpm (10g)
Depth of soil from channel top: 41mm

Calculated shear stress calculated from soil strength profiles shown in section 5.1 which are formed from the measured soil strength values.

Sample	Depth below clay surface / cm	Measured shear stress / kPa	Calculated shear stress / kPa	Comments
1	0	0	-	Soil profile
2	2	0.6	-	Soil profile
3	3.9	1.4	-	Soil profile
4	5.8	2	-	Soil profile
5	8.3	2.6	-	Soil profile
6	4.5	-	1.48	1st pasta break depth
7	4.4	-	1.45	2nd pasta break depth
8	4.3	-	1.42	3rd pasta break depth
10	5.6	-	1.94	Depth of anchor trail

Table 12: Table of experimental observations and readings, experiment 9

Successful experiment, due to path of anchor it only broke three pieces of pasta. Due to the low speed and small penetration depth the anchor fell out as the speed was reduced at the end of testing leading to no in-situ depth measurements.

Average penetration depth: 44mm
Average undrained shear strength at penetration depth: 1.45kPa

10 Appendix III

10.1 Comments on initial risk assesment

The initial risk assesment identified some risks associated with the use of a centrifuge. Primarily these were the dangers of trapping limbs or clothes in the centrifuge or of parts escaping when it was in motion. These were correctly identified and safety measures such as using the necessary screens and safety stops were implemented successfully.

However two additional hazards became apparent:

- Working at heights. The centrifgue top is located two metres above the ground, to prevent clay falling out it is necessary to change the apparatus when it is in its elevated position. Although there is a safe working platform this can often become slippy with clay and water, care must be taken and tools stored safely away to ensure a fall doesn't occur.
- Manual lifting. To load the clay slurry into the centrifuge, it must be lifted in 5L buckets from the floor to the feeding funnel, 2m above the floor. Although it is only a relatively small load, this procedure must be carried out more than 20 times. This is a physically demanding task and care must be taken to avoid injury.